



Published in final edited form as:

J Mol Cell Cardiol. 2016 October ; 99: 100–112. doi:10.1016/j.yjmcc.2016.08.009.

Loss of Myocardial Retinoic Acid Receptor α Induces Diastolic Dysfunction by Promoting Intracellular Oxidative Stress and Calcium Mishandling in Adult Mice

Sen Zhu¹, Rakeshwar S. Guleria^{1,2,*}, Candice M. Thomas¹, Amanda Roth¹, FNU Gerilechaogetu¹, Rajesh Kumar^{1,2}, David E. Dostal^{1,2}, Kenneth M. Baker¹, and Jing Pan^{1,2,*}

¹Department of Medicine, College of Medicine, Texas A&M University Health Science Center; Central Texas Veterans Health Care System; Baylor Scott & White Health; Temple, TX

²Department of Medical Physiology, College of Medicine, Texas A&M University Health Science Center; Central Texas Veterans Health Care System; Baylor Scott & White Health; Temple, TX

Abstract

Retinoic acid receptor (RAR) has been implicated in pathological stimuli-induced cardiac remodeling. To determine whether the impairment of RAR α signaling directly contributes to the development of heart dysfunction and the involved mechanisms, tamoxifen-induced myocardial specific RAR α deletion (RAR α KO) mice were utilized. Echocardiographic and cardiac catheterization studies showed significant diastolic dysfunction after 16 wks of gene deletion. However, no significant differences were observed in left ventricular ejection fraction (LVEF), between RAR α KO and wild type (WT) control mice. DHE staining showed increased intracellular reactive oxygen species (ROS) generation in the hearts of RAR α KO mice. Significantly increased NOX2 (NADPH oxidase 2) and NOX4 levels and decreased SOD1 and SOD2 levels were observed in RAR α KO mouse hearts, which were rescued by overexpression of RAR α in cardiomyocytes. Decreased SERCA2a expression and phosphorylation of phospholamban (PLB), along with decreased phosphorylation of Akt and Ca²⁺/calmodulin-dependent protein kinase II δ (CaMKII δ) was observed in RAR α KO mouse hearts. Ca²⁺ reuptake and cardiomyocyte relaxation were delayed by RAR α deletion. Overexpression of RAR α or inhibition of ROS generation or NOX activation prevented RAR α deletion-induced decrease in SERCA2a expression/activation and delayed Ca²⁺ reuptake. Moreover, the gene and protein expression of RAR α was significantly decreased in aged or metabolic stressed mouse hearts. RAR α deletion accelerated the development of diastolic dysfunction in streptozotocin (STZ)-induced type 1 diabetic mice or in high fat diet fed mice. In conclusion, myocardial RAR α deletion promoted diastolic dysfunction, with a relative preserved LVEF. Increased oxidative stress have an important role in the decreased expression/activation of SERCA2a and Ca²⁺ mishandling in RAR α KO mice,

* Address correspondence to: Jing Pan, MD, PhD, jpan@medicine.tamhsc.edu; Tel. 254-743-2461; Rakeshwar Guleria, rsguleria@medicine.tamhsc.edu; Tel. 254-743-1593. Fax. 254-743-0165. Department of Medical Physiology, College of Medicine, Texas A&M University Health Science Center. 1901 South 1st Street, Bldg. 205, Temple, Texas.

Publisher's Disclaimer: This is a PDF file of an unedited manuscript that has been accepted for publication. As a service to our customers we are providing this early version of the manuscript. The manuscript will undergo copyediting, typesetting, and review of the resulting proof before it is published in its final citable form. Please note that during the production process errors may be discovered which could affect the content, and all legal disclaimers that apply to the journal pertain.

Disclosures: None declared

which are major contributing factors in the development of diastolic dysfunction. These data suggest that impairment of cardiac RAR α signaling may be a novel mechanism that is directly linked to pathological stimuli-induced diastolic dysfunction.

Keywords

Retinoic acid receptor; diastolic dysfunction; oxidative stress; calcium handling

1. INTRODUCTION

Heart failure (HF) is the leading cause of morbidity and mortality that affects 5.3 million Americans, with increasing prevalence and high hospitalization, but poor diagnostic and treatment options. Evidently, more than 50% of HF patients are diagnosed with diastolic HF, which is prevalent in aging, hypertensive, obese or diabetic patients [1, 2]. Approximately 30–50% of diabetic patients with the typical clinical signs of HF, suffer primarily from diastolic HF [3]. There is no clear guideline-based therapeutic strategy to effectively manage diastolic HF, due to the limited understanding of the pathophysiological mechanisms. Oxidative stress have been linked to the development of chronic heart failure and conditions, like hypertension and myocardial infarction, that predispose to HF [4]. Numerous experimental studies have provided direct molecular evidence for an etiological role of reactive oxygen species (ROS) in HF [5, 6]. However, clinical trials of antioxidant vitamins have been singularly unsuccessful [7], suggesting that the relationship between oxidative stress and HF or its antecedent conditions is more complex, and understanding the initiation of oxidative stress as well as its downstream effects on cellular function would be significant for identifying the underlying mechanisms of HF and developing more specific targeted therapies.

The nuclear retinoic acid receptor (RAR) and retinoid X receptor (RXR) mediate most of the cellular functions of retinoic acid (RA) [8]. RAR is activated when heterodimerizing with RXRs. We have demonstrated that RAR α is one of the receptor subtypes that are abundantly expressed in cardiomyocytes [9, 10]. Activation of RAR/RXR-mediated signaling attenuates hypertrophic stimuli-induced cardiac remodeling, through regulation of oxidative stress/MAP kinase cascades and the renin-angiotensin system [10–15]. Recently, we reported that activation of RAR α signaling prevented high glucose and diabetes-induced diastolic dysfunction, through inhibition of intracellular ROS generation and NF- κ B signaling-mediated inflammatory responses [9, 16, 17]. These results suggested that RAR α -mediated signaling has an important role in regulation of cardiac oxidative stress in response to pathological stimuli, which may serve as a critical mechanism in the development of diastolic dysfunction and HF. Up to date, a majority of studies in relate to the role of RAR/RXR in regulation of adult heart function have utilized RAR pan or subtype selective ligands or antagonists, due to heart malformation and poor survivability of genetic models of RAR deletion. The non-specificity of ligands toward other nuclear receptors results in inaccuracy in interpreting the functional role of RAR α in regulation of cellular function in heart. Therefore, studies with inducible receptor knockout models are critical to understand the functional role of RAR α in regulation of cardiac oxidative stress and heart function.

Using a mouse model with tamoxifen-induced cardiac specific RAR α gene deletion, we investigated the cardiac phenotype, systemic hemodynamics as well as signaling mechanisms in RAR α KO mice as compared to WT littermates. We observed that RAR α KO mice have an impaired LV diastolic function with preserved EF, which is associated with increased oxidative stress and impaired calcium reuptake and cardiomyocyte relaxation. RAR α deletion-induced increase in intracellular ROS has a critical role in the decreased expression/activation of SERCA2a and calcium mishandling. The gene and protein expression of RAR α was decreased in aged mouse hearts and metabolic stressed mouse hearts. Gene deletion of RAR α promoted the development of diastolic dysfunction at early stage in STZ-induced type 1 diabetic mice and high fat diet fed mice. These data suggest that loss of myocardial RAR α signaling is directly associated with the development of diastolic dysfunction, which provide new insights into how cardiac RAR α expression/activation impacts heart function and the development of HF.

2. RESEARCH DESIGN AND METHODS

A detailed Methods section is available in the Online Data Supplement.

2.1 Experimental model

Animal use was approved by the Institutional Animal Care and Use Committee of the Texas A&M Health Science Center and conformed to the *Guide for the Care and Use of Laboratory Animals*, published by the National Institutes of Health (NIH Pub. No. 85-23, 1996). Cardiac specific RAR α gene deletion (RAR α KO) was achieved by tamoxifen injection in male α -MHC-Cre-RAR $\alpha^{fl/fl}$ mice at the age of 6 wks (weeks). Age-matched α -MHC-Cre-RAR $\alpha^{fl/fl}$ mice treated with vehicle or RAR $\alpha^{fl/fl}$ mice, received tamoxifen at same time were used as wild type (WT) control. One set of mice were sacrificed at 20 wks (young group, n=20/group) and another at 64 wks (aged group, n=20/group) after tamoxifen injection. Streptozotocin (STZ) induced type 1 diabetic model was generated by injection of STZ (60 mg/kg/day) intraperitoneally, for 5 days, after 4 wks of tamoxifen injection in RAR α KO mice and at age of 10 wks in WT mice (n=12). Mice with fasting blood glucose 250 mg/dL were used for the study. Mice received buffered saline alone were used as control. Another set of RAR α KO and WT mice (n=8) were fed with high fat diet (HFD, 60% of calories from fat; Harlan Teklad, WI) or normal chaw for 12 wks. Gene deletion was induced the same day as initiation of HFD feeding (age of 6 wks).

2.2 Echocardiographic measurements and hemodynamic studies

Echocardiograms were performed using a VisualSonic Vevo 2100 system equipped with a 40-MHz probe, every 4 wks until 64 wks after gene deletion. Mice were anesthetized with 3–5% isoflurane that was reduced to 1.5% to maintain the heart rate between 400–450 beats per minute. The ECG was monitored continuously in real time. The echo-table temperature was controlled at 39°C. The heart was imaged in the 2-dimensional, short-axis and 4 chamber views [18, 19]. Two-dimensional imaging, tissue Doppler and M-Mode measurements were performed to analyze cardiac structural and functional changes. All mice recovered from the procedure without signs of distress. LV catheterization was

performed using a 1.2-F microconductance pressure-volume catheter (Transonic Systems Inc, NY) at 20 wks to evaluate LV systolic and diastolic function [19].

2.3 Isolation of neonatal and adult mouse cardiomyocytes

Neonatal mouse cardiomyocytes were isolated and cultured from 1–3 day old $RAR\alpha^{fl/fl}$ mice, as described previously [20]. $RAR\alpha$ gene deletion was induced by transfecting cells with adenovirus-mediated overexpression of Cre recombinase (AdCre, 50 MOI). Cells transfected with AdGFP were used as wild type control. Overexpression of $RAR\alpha$ was induced by adenovirus-mediated wild-type $RAR\alpha$ (Ad $RAR\alpha$) transfection.

Adult mouse cardiomyocytes were isolated from WT and $RAR\alpha$ KO mice at 20 wks, as previously described with some modifications [21]. The isolated cardiomyocytes were used immediately for Ca^{2+} transients and twitch analysis or cultured for other experiments.

2.4 Intracellular Ca^{2+} transients and twitch analysis

Isolated adult mouse cardiomyocytes were loaded with 10 μ M/L Fura-2-AM and placed on the stage of an inverted microscope. To evoke electrically stimulated Ca^{2+} transients and cell contraction, cells were field stimulated at 0.2 Hz until the response reached steady state. Fluorescence measurements were recorded with a dual-excitation fluorescence photomultiplier system (IonOptix, MA). Calcium transients and twitch analysis were assessed using the IonWizard Transient analysis program and video-based edge-detection, respectively. Sarcoplasmic reticulum (SR) Ca^{2+} loading capacity was assessed with a brief pulse of caffeine to induce SR Ca^{2+} release. In some cases, cells were treated with NAC (5 mmol/L, 30 min) before the experiments began. Data were recorded from at least 15 cells per heart and for at least 5 hearts per group.

2.5 Statistical analysis

All data are expressed as the mean \pm SEM. Comparisons between groups were performed using the Student *t* test, Kruskal–Wallis test, or 1-way ANOVA, followed by the Tukey post-hoc test, where appropriate. A *P* value <0.05 was considered statistically significant.

3. RESULTS

3.1 Gene deletion of $RAR\alpha$ impairs myocardial relaxation and diastolic function

Cardiac specific $RAR\alpha$ deletion was achieved by tamoxifen injection, at the age of 6 wks. PCR data showed that gene deletion of $RAR\alpha$ occurred only in hearts following tamoxifen injection (Fig. 1A). Cardiac protein expression of $RAR\alpha$ was significantly decreased in hearts of $RAR\alpha$ KO mice and in cardiomyocytes isolated from $RAR\alpha$ KO mice, compared to WT (Fig. 1B and C). The expression of other subtype receptors ($RAR\beta$, $RXR\alpha$ and $RXR\beta$) in hearts of $RAR\alpha$ KO and WT mice was similar (Supplemental Fig. 1), suggesting that there was no compensatory expression following deletion of $RAR\alpha$. $RAR\alpha$ deletion had no effect on mean blood pressure and heart rate (Supplement table 1). Heart function was monitored by echocardiography (monthly for 64 wks) and an invasive hemodynamic assessment (after 20 wks of gene deletion). In $RAR\alpha$ KO mice, systolic function was well preserved, as indicated by left ventricular ejection fraction (EF%; 65 ± 2.9 in WT vs 67 ± 1.7 in $RAR\alpha$ KO,

at 64 wks) and fractional shortening (FS%, 35.9 ± 2.3 in WT vs 36.5 ± 1.3 in RAR α KO), which were comparable with WT littermates (Fig. 1D and supplemental Fig. 2). Hemodynamic studies performed at 20 wks showed similar levels of dP/dt_{\max} , $dP/dt_{\max}/EDV$ and EF% (systolic function indices) in WT and RAR α KO mice (Fig. 1G and supplemental table 1). Diastolic dysfunction developed after 8–12 wks of gene deletion, with increased isovolumetric relaxation time (IVRT) and decreased tissue Doppler early diastolic mitral annular velocity (TDI E') (Supplemental Fig. 3). RAR α KO mice exhibited significant diastolic dysfunction after 16 wks, as evidenced by a decreased E/A ratio, TDI E' (estimate LV longitudinal myocardial relaxation) and increased IVRT, DT (deceleration time of the E-wave) and E/E' ratio (estimate left atrial filling pressure), compared to WT mice (Fig. 1E and supplemental Fig. 3). Hemodynamic studies (Fig. 1H–J and supplemental table 1) showed consistent data, with reduced dP/dt_{\min} , decreased dPR ratio (index of heart's ability to relax to its maximum rate of pressure development) and increased Tau (isovolumic LV relaxation time constant). A mild increase in LVEDP (LV end-diastolic pressure) was observed in RAR α KO mice, but did not reach statistical significance, compared to WT. Decreased LV cardiac output (CO) was only observed after 56 wks (Fig. 1F and Supplemental Fig. 3), which is consistent with the increased lung weight in RAR α KO mice after 64 wks of gene deletion (Supplemental table 2). These findings suggest that lack of RAR α signaling impairs myocardial relaxation, resulting in the development of diastolic dysfunction and HF.

3.2 Role of RAR α in cardiac hypertrophy and fibrosis

The hypertrophic structural changes were only observed in aged RAR α KO mice, as evidenced by increased heart weight to tibia length ratio (HW/TL, 0.084 ± 0.002 g/cm versus 0.072 ± 0.002 g/cm in WT, $p < 0.05$), LV/TL ratio (0.067 ± 0.002 g/cm versus 0.053 ± 0.003 g/cm in WT, $p < 0.05$) and cardiomyocyte cross sectional area (CSA, 1.903 ± 0.068 versus 1.083 ± 0.09 in WT, $p < 0.05$) at 64 wks, but not in young (20 wks) mice (Fig. 2A–C, Supplemental table 2). Echocardiographic studies confirmed that significant cardiac hypertrophy developed after 52 wks of gene deletion, by increased thickness of LV posterior wall end diastole (LVPWd, 0.79 ± 0.03 mm versus 0.598 ± 0.03 mm in WT, $p < 0.05$) and interventricular septal end diastole (IVSd, 0.67 ± 0.02 mm versus 0.54 ± 0.05 mm in WT, $p < 0.05$), compared to WT mice (Fig. 2D and supplement Fig. 2). LV internal diameter end diastole (LVIDd) and end systole (LVIDs) significantly decreased at 64 wks (LVIDd: 3.43 ± 0.099 mm versus 4.06 ± 0.095 mm in WT; LVIDs: 2.27 ± 0.095 mm versus 2.99 ± 0.091 mm in WT, $p < 0.05$, Supplement Fig. 2), suggesting that RAR α deletion induced concentric cardiac hypertrophy in aged mice. Gene expression of atrial natriuretic peptide (ANP), brain natriuretic peptide (BNP) and β -myosin heavy chain (β -MHC) was significantly increased at 20 wks, however, there were no significant changes in the expression of BNP and β -MHC in aged (64 wks) RAR α KO mouse hearts, compared to WT (Fig. 2E). The protein expression of cardiac β -MHC was significantly increased at 20 wks in RAR α KO mice, compared to WT (Fig. 2F). Increased protein expression of β -MHC was also observed in aged WT and RAR α KO mice ($p < 0.05$, vs young group), however, there was no difference between WT and RAR α KO mice ($p > 0.05$). Aging-induced increase in β -MHC expression in WT mice may attenuate the difference between WT and RAR α KO mice. Masson's trichrome staining showed significant increased cardiac fibrosis in aged WT and RAR α KO mouse hearts,

compared to young mice; however, no significant difference was observed between WT and RAR α KO mice (supplemental Fig. 4). Consistent data were observed by hydroxyproline assay. Hydroxyproline serves to stabilize the helical structure of collagen. Hydroxyproline is largely restricted to collagen, the measurement of hydroxyproline levels can be used as an indicator of collagen content. There was no significant increase in LV hydroxyproline levels at 20 wks, in RAR α KO mice, compared to WT. However, the hydroxyproline levels markedly increased in aged WT (0.591 ± 0.037 $\mu\text{g}/\text{mg}$ LV, vs 0.438 ± 0.013 $\mu\text{g}/\text{mg}$ LV, in WT at 20 wks) and RAR α KO mice (0.637 ± 0.044 $\mu\text{g}/\text{mg}$ LV, vs 0.452 ± 0.070 $\mu\text{g}/\text{mg}$ LV, in RAR α KO at 20 wks). There was no significant difference between WT and RAR α KO mice (supplemental Fig. 4), suggesting that aging is related to the increased collagen content in 64 wks of WT and RAR α KO mice. Fibrotic gene expression of collagen type I and TGF- β were similar in young and aged WT and RAR α KO mice (Fig. 2E). These data suggest that RAR α deletion has no significant effect on cardiac fibrosis.

3.3. Gene deletion of RAR α promotes cardiac oxidative stress

To determine the role of RAR α in regulation of cardiac oxidative stress, dihydroethidium (DHE) staining of LV sections, a relatively specific indicator of O $_2^{\cdot-}$, was performed after 20 and 64 wks of gene deletion. A significantly increased DHE staining was observed in RAR α KO mouse hearts, at 20 and 64 wks, compared to WT, suggesting that increased intracellular ROS generation following RAR α deletion (Fig. 3A and B). RAR α gene deletion also promoted aging-induced ROS generation, as evidenced by significantly increased DHE staining in aged RAR α KO mouse hearts, compared to young (20 wks) mice. Reduced glutathione (GSH) is a major tissue antioxidant and that GSSG (glutathione disulfide), the oxidized form of glutathione, will accumulate in response to oxidative stress. Thus, the ratio of GSH/GSSG within cells is often used as a measure of cellular oxidative stress. A significantly decreased GSH/GSSG ratio was observed in RAR α KO mice, compared to age matched WT (Fig. 3C). Compared to young mice, aged WT and RAR α KO mice showed significantly reduced GSH/GSSG ratio ($p<0.05$), suggesting that increased oxidative stress in aged hearts, and that gene deletion of RAR α further promoted aging-induced oxidative stress. Increased ROS in the failing heart are mainly due to impaired antioxidant capacity, such as reduced activity of SOD and catalase, or stimulation of enzymatic sources, in which nonphagocytic NAD(P)H oxidases (NOX) are major enzymes responsible for production of O $_2^{\cdot-}$. We then determined the mechanism of RAR α deletion-induced ROS generation. Gene and protein expression of NOX2, NOX4, SOD1 and SOD2 was analyzed. Significantly increased gene and protein expression of NOX2 and NOX4 and decreased SOD1 and SOD2 were observed in RAR α KO mouse hearts, at 20 and 64 wks, compared to age matched WT (Fig. 3D–F). RAR α deletion further reduced gene and protein expression of SOD1 and SOD2 in aged mice, suggesting that RAR α deletion had additional deleterious effect on aging-induced impairment of anti-oxidant defense system. A significantly decreased gene and protein expression of SOD2 was also observed in aged WT mice ($p<0.05$, compared to young WT). In combine with the increased DHE staining and decreased GSH/GSSG ratio in aged WT mice, it is likely that decreased SOD2 has an important role in aging-induced myocardial oxidative stress.

We further confirmed the role of RAR α in regulation of oxidative stress in cultured neonatal and adult mouse cardiomyocytes (Supplemental Fig. 5). Neonatal cardiomyocytes isolated from RAR $\alpha^{fl/fl}$ mouse heart were transfected with adenovirus-mediated overexpression of Cre recombinase (AdCre) to induced gene deletion, and then transfected with or without wildtype RAR α (AdRAR α) to re-expression of RAR α . Significantly increased DHE staining was observed in cardiomyocytes with RAR α deletion, which was inhibited by overexpression of RAR α (supplemental Fig. 5A and B). Adult cardiomyocytes isolated from WT and RAR α KO mouse heart at 20 wks showed consistent data. The increased protein expression of NOX2, NOX4 and decreased SOD1 and SOD2 were observed in cardiomyocytes from RAR α KO mice, and that overexpression of RAR α rescued the decreased SOD1 and SOD2 level and restored the increased NOX2 and NOX4 level to normal (supplemental Fig. 5C and D). These results suggest that lacking of RAR α signaling promotes excessive ROS generation, through upregulation of NOX2 and NOX4 and decreasing SOD1 and SOD2-mediated anti-oxidant defense system.

3.4. RAR α deletion inhibits the expression/activation of SERCA2a

Diastolic intracellular calcium handling is a major determinant of LV relaxation. Failure to properly recycle Ca²⁺ through the sarcoplasmic reticulum (SR) results in severe impairment of myocardial relaxation. It has been reported that sarcoplasmic reticulum Ca²⁺ ATPase2a (SERCA2a) is the main mechanism for removing Ca²⁺ from cytosol into SR (92% of the calcium in mouse and 75% in human) in cardiomyocytes [22]. SERCA2a activity is tightly regulated by phospholamban (PLB) [23]. PLB reduces the affinity of SERCA2a for Ca²⁺. This inhibitory effect is released upon phosphorylation at Ser16 by PKA or Thr17 by calcium/calmodulin dependent protein kinase (CaMKII) or Akt [24, 25]. PLB exists as monomeric, dimeric and pentameric forms (~6 to ~30KD) [26, 27]. The monomers represent the active fraction of PLB by attenuating the activity of the Ca²⁺ pump, and pentamers are involved in modify the phosphorylation status of PLB, function as a regulator of PLB activity [28–30]. We observed decreased protein expression of SERCA2a and phosphorylation of PLB (at both Ser16 and Thr17 sites) in RAR α KO mouse hearts, along with unchanged total PLB levels, which resulted in increased PLB/SERCA2a ratio, compared to WT mice, at 20 wks (Fig. 4A and B) and 64 wks (supplemental Fig. 7A). Multiple bands that represent monomeric and pentameric form of PLB were observed with long time exposure (Supplemental Fig. 6). The phosphorylation of PLB at Ser16 (~6, ~14 and ~24 KD) and Thr 17 (~6 and ~14 KD) was detected in the hearts of WT mice, and the monomeric form (~6KD) was abundantly expressed in myocardium. RAR α deletion attenuated the phosphorylation of monomeric and pentameric form of PLB. These data suggest that RAR α deletion inhibits SERCA2a activity through regulation of the phosphorylation of PLB. The phosphorylation of Akt was decreased in RAR α KO mouse hearts. Interestingly, the total protein level of CaMKII δ significantly decreased following RAR α deletion. Though the relative phosphorylation of CaMKII δ (against total CaMKII δ) was increased, the overall phosphorylation of CaMKII δ (against total α -tubulin) was decreased in RAR α KO mouse hearts.

The effect of RAR α deletion on SERCA2a expression/activation was further confirmed in cultured neonatal and adult mouse cardiomyocytes. As shown in Fig. 4C, deletion of RAR α

resulted in decreased protein expression of SERCA2a and phosphorylation of PLB (Ser16 and Thr17), and increased PLB/SERCA2a ratio, suggesting inhibited SERCA2a activity. Overexpression of RAR α prevented the decreased SERCA2a activity (quantification data shown in supplemental Fig. 7B). In consistent with the *in vivo* data, decreased phosphorylation of Akt and the expression/phosphorylation of CaMKII δ were observed in cardiomyocytes with RAR α deletion, which were rescued by overexpression of RAR α (Fig 4C and supplemental Fig. 7B). Adult RAR α KO cardiomyocytes were cultured and pretreated with specific activators for PKA (8-Br-cAMP), CaMKII (activated CaMKII) or Akt (SC79). We observed that RAR α deletion-induced decrease in the phosphorylation of PLB at Ser16 was restored by 8-Br-cAMP, and the reduced phosphorylation of PLB at Thr17 was restored by activated CaMKII and SC79 (supplemental Fig. 8A). These data suggest that RAR α deletion may impair the phosphorylation of PKA, CaMKII δ or Akt, which results in inhibition of the phosphorylation of PLB, leading to increased PLB/SERCA2a ratio and SERCA2a inactivation.

3.5. Oxidative stress is involved in RAR α deletion-induced downregulation of SERCA2a and calcium mishandling

Neonatal mouse cardiomyocytes were treated with NAC (N-acetyl-L-cysteine, a ROS scavenger) for 2 and 24 h, after RAR α deletion, role of oxidative stress in RAR α deletion-induced downregulation/inactivation of SERCA2a was determined. RAR α deletion-induced inhibition of the expression of SERCA2a and phosphorylation of PLB (Ser16 and Thr17), CaMKII δ and Akt were prevented by 24 h of NAC treatment (Fig. 5A and B). Moreover, inhibition of NOX activation by VAS2870 in adult RAR α KO cardiomyocytes, also rescued the decreased expression and phosphorylation of CaMKII δ (Supplemental Fig. 8B). These results suggest that RAR α deletion-induced oxidative stress has an important role in the downregulation/inactivation of SERCA2a in cardiomyocytes.

We further determined the role of oxidative stress in Ca²⁺ handling and cell contractility. Adult cardiomyocytes isolated from WT and RAR α KO mouse hearts, at 20 wks, were cultured and treated with or without NAC for 30 min, cardiomyocyte contractile activity and Ca²⁺ cycling determined. As shown in table 1, we observed that myocyte shortening was depressed in RAR α KO myocytes, in response to 0.2 Hz stimulation, with a maximal inhibition of 38% in peak shortening and 46% in +dL/dt (maximal velocities of shortening), compared to WT. Cardiomyocyte relengthening (relaxation) was significantly impaired in RAR α KO cardiomyocytes, as characterized by slowed -dL/dt (maximum velocity of relengthening), increased TR50, TR90 (time to 50% and 90% of relengthening, respectively) and Tau, suggesting that RAR α deletion impairs cardiomyocyte relaxation and cell contractility in response to stress stimulation. RAR α deletion had no effect on calcium release, as there were no significant changes in the resting diastolic [Ca²⁺]_i, the peak rate of calcium release (dep v), the time to maximal departure velocity (dep v t) and time to 50% of the peak height in RAR α KO cardiomyocytes, compared to WT. SR Ca²⁺ load was slightly decreased in RAR α KO cardiomyocytes, but, didn't reach statistical significance, compared to WT. Importantly, Ca²⁺ reuptake was impaired in RAR α KO cardiomyocytes, as demonstrated by decreased peak rate of decline of Ca²⁺ transients (return velocity, ret v), increased time to 50% and 90% of the base line (T50CR and T90CR, respectively) and

prolonged tau (calcium transient decay). These data suggest that delayed Ca^{2+} reuptake is the main mechanism contributing to $\text{RAR}\alpha$ deletion-induced impairment of relaxation. $\text{RAR}\alpha$ deletion-induced impairment of calcium reuptake and cell relaxation was significantly improved after NAC treatment. These data suggest that oxidative stress has a major contribution in $\text{RAR}\alpha$ deletion-induced calcium mishandling and impaired relaxation.

3.6. Cardiac expression of $\text{RAR}\alpha$ has an important role in aging and metabolic stress-induced diastolic dysfunction and oxidative stress

We have reported that decreased cardiac expression of $\text{RAR}\alpha$ in ZDF rats, along with diastolic dysfunction and increased oxidative stress, which were ameliorated by $\text{RAR}\alpha$ selective ligand [17]. Thus, we further analyzed the contribution of $\text{RAR}\alpha$ in the development of diastolic dysfunction in aging and metabolic disorder mouse models. Hearts were collected from young (age of 26 wks), aged (age of 70 wks), 20 wks of STZ-induced type 1 diabetic or HFD-fed mice, gene and protein expression of $\text{RAR}\alpha$ was determined. As shown in Fig 6A and B, cardiac gene and protein expression of $\text{RAR}\alpha$ were significantly decreased in aged, STZ-induced diabetic and HFD-fed hearts. Next, we analyzed heart functional changes in these mouse models. Increased IVRT and decreased TDI E' were observed in aged mice, compared to young mice, suggesting that diastolic dysfunction developed with aging (supplemental Fig. 3). $\text{RAR}\alpha$ deletion also promoted the ROS generation in aged mouse hearts (Fig. 3 A–C). Decreased E/A ratio and increased DT were observed in STZ-treated or HFD-fed $\text{RAR}\alpha$ KO mice, at 4 wks, compared to STZ-treated or HFD-fed WT mice (Fig. 6C and D), suggesting that deletion of $\text{RAR}\alpha$ accelerated metabolic stress-induced development of diastolic dysfunction.

Next, we determined the effect of $\text{RAR}\alpha$ deletion on cardiac oxidative stress and the expression of SERCA2a in STZ-induced type 1 diabetic mice. As shown in Fig. 7A and B, DHE staining increased dramatically in STZ- $\text{RAR}\alpha$ KO mice, compared to STZ-WT and non-diabetic $\text{RAR}\alpha$ KO mice. $\text{RAR}\alpha$ deletion induced a significant decrease in SOD1 and SOD2 protein levels and increase in NOX2 and NOX4 expression in both diabetic and non-diabetic mice, compared to WT-STZ mice (Fig. 7C and D). Significantly decreased expression of SERCA2a, phosphorylation of PLB and increased PLB/SERCA2a ratio were observed in STZ- $\text{RAR}\alpha$ KO mice, compared to STZ-WT or non-diabetic $\text{RAR}\alpha$ KO mice. These data suggest that downregulated expression and/or activation of $\text{RAR}\alpha$ is involved in cardiac oxidative stress and calcium mishandling, which has an important role in the early development of diastolic dysfunction in mice with metabolic stress.

4. DISCUSSION

This study provides the first evidence that deletion of $\text{RAR}\alpha$ in adult mouse myocardium causes diastolic dysfunction with a relatively preserved LVEF and that downregulation of cardiac $\text{RAR}\alpha$ is directly associated with the development of diastolic dysfunction, in aging and metabolic stressed hearts. $\text{RAR}\alpha$ deletion promotes intracellular ROS generation and oxidative stress, through increasing the expression of NOX2 and NOX4 and inhibiting SOD1 and SOD2 levels; and that increased oxidative stress has a critical role in $\text{RAR}\alpha$

deletion-induced SEARCA2a inactivation, calcium mishandling and subsequent diastolic dysfunction.

The importance of RAR/RXR signaling pathway has been evidenced by heart malformation and early death in constitutive RAR α and RXR α knockout mice [31–33]. The high degree of conservation of RAR and RXR across vertebrates and specific patterns of expression during embryogenesis and in adult tissues, suggest that each of the receptor subtypes performs a specific function [34]. We have demonstrated that activation of RAR by receptor selective ligands inhibits mechanical stretch, angiotensin II, pressure overload or metabolic stress-induced cardiac hypertrophy, fibrosis and heart dysfunction, *in vitro* and *in vivo* [9, 10, 14, 15, 17]. Silencing the expression of RAR α in cardiomyocytes promoted cell apoptosis [9]. Importantly, RAR α , as one of the major subtype receptors expressed in heart, its expression and transcriptional activation were significantly inhibited in high glucose-stimulated cardiomyocytes and in the hearts of Zucker diabetic fatty (ZDF) rats [9, 17, 35]. Moreover, we found that gene and protein expression of RAR α was significantly decreased in aged myocardium and in the hearts of STZ-induced type 1 diabetic mice or HFD fed mice, in the present studies. These data strongly suggest that impairment of RAR α signaling may be directly associated with the development of heart dysfunction in response to various pathological stimuli. Using an inducible cardiac specific knockout mouse model, we provided the first evidence that loss of RAR α -mediated signaling resulted in diastolic dysfunction, with preserved LVEF in adult mice. Echocardiographic and hemodynamic studies demonstrated that cardiac specific deletion of RAR α induced decreased E/A ratio, TDI E', dP/dt_{min} and increased E/E', IVRT, DT and Tau, which indicating prolonged LV relaxation and increased left atrial filling pressure. RAR α deletion significantly impaired cardiomyocyte relaxation, as evidenced by slowed $-dL/dt$, increased TR50, TR90 and Tau in adult cardiomyocytes isolated from RAR α KO mouse hearts. RAR α deletion had no significant effect on LV systolic function, as evidenced by unchanged LVEF%, FS% and dP/dt_{max}, compared to WT mice, suggesting that impairment of RAR α signaling leads to the development of diastolic dysfunction, with preserved systolic function. Though the *in vivo* functional analysis showed normal systolic function in RAR α KO mice, *in vitro* studies showed that cardiomyocyte contractility was decreased in isolated RAR α KO cardiomyocytes, in response to 0.2 Hz electrical stimulation, suggesting that LV systolic function is relatively preserved in RAR α KO mice. This is consistent with clinical studies which have shown that the subtle abnormalities in resting systolic performance in patients with diastolic heart failure become more dramatic during physiological stress [36, 37]. The importance of RAR α in regulation of heart function was further demonstrated in metabolic stressed mouse models. Gene deletion of RAR α accelerated the development of diastolic dysfunction, at early stage (4 wks after gene deletion and challenged with metabolic stress), in STZ-induced type 1 diabetic mice and HFD fed mice, compared to WT mice, where diastolic dysfunction developed around 12–16 wks in response to metabolic stress. In combine with the decreased cardiac gene and protein expression of RAR α in STZ or HFD mice, it is clear that downregulation of cardiac RAR α signaling is directly linked to the development of diastolic dysfunction and heart failure, in response to pathological stimuli.

Cardiac hypertrophy contributes to the impaired active relaxation, increased passive stiffness of the LV and subsequent diastolic dysfunction and HF [38]. RAR α deletion-induced

diastolic dysfunction was observed after 8–12 wks of gene deletion, along with increased gene expression of ANP, BAP and β -MHC (markers of cardiac hypertrophy and HF), however, the hypertrophic structural changes were only observed after 52 wks of gene deletion, suggesting that RAR α deletion induced early development of diastolic dysfunction in the absence of hypertrophy. This hypertrophy independent diastolic dysfunction has been reported in population-based clinical studies, which have shown that many patients with diastolic HF have either concentric remodeling in the absence of hypertrophy, or even normal LV geometry [39, 40]. Cardiac fibrosis and increased collagen turnover also contribute to the increased myocardial stiffness and diastolic dysfunction [41, 42]. However, the fibrotic gene expression (TGF β and collagen type I) and collagen levels are comparable in WT and RAR α KO mice, suggesting that RAR α deletion-induced diastolic dysfunction may be not related to increased myocardial fibrosis. Determining the effect of RAR α on collagen cross-linking and turnover (activity of matrix metalloproteinases and tissue inhibitor of metalloproteinases) will provide more evidence to clarify the direct linkage between fibrosis and RAR α deletion-induced diastolic dysfunction.

Cardiac myosin binding protein C (cMyBP-C), a cardiac-specific thick filament accessory proteins [43] that can modulate cross-bridge attachment/detachment cycling process by its phosphorylation status, appears to be involved in the diastolic dysfunction associated with diastolic HF. Large amount of animal and human studies have shown the importance of cMyBP-C in regulation of LV relaxation and diastolic function [44–48]. Mutations in cMyBP-C induce diastolic dysfunction in patients with hypertrophic cardiomyopathy, which is independent of hypertrophy [44, 45]. Loss of cMyBP-C in mice causes diastolic dysfunction [46] and that conditional cMyBP-C knockout induces diastolic dysfunction before the onset of cardiac hypertrophy [47]. RAR α deletion induced diastolic dysfunction phenotype is similar with the functional changes demonstrated in cMyBP-C knockout mice. Recent studies further indicated that posttranslational modification of cMyBP-C is directly associated with diastolic dysfunction. Oxidative stress-induced *S*-glutathionylation of cMyBP-C induces Ca²⁺ sensitization and a slowing of cross-bridge kinetics, leading to diastolic dysfunction [49, 50]. The phosphorylation of cMyBP-C by PKA and CaMKII δ [51–53] has been implicated in regulation of diastolic function [19, 54]. Unphosphorylated cMyBP-C appears to repress cross-bridge attachment and detachment, results in impaired relaxation. We observed significantly increased ROS generation and decreased PKA/CaMKII δ activation in RAR α KO mice (as discussed below), thus, the posttranslational modification of cMyBP-C may be involved in RAR α deletion-induced diastolic dysfunction, through inhibition of the phosphorylation of cMyBP-C or increasing the *S*-glutathionylation of cMyBP-C. Further study is required to clarify the role of cMyBP-C in RAR α deletion-induced diastolic dysfunction.

It has been reported that decreased SERCA2a function and reduced Ca²⁺ uptake activity is associated with Ca²⁺ mishandling and slow relaxation in diastolic dysfunction [55–57]. Decreased Ca²⁺ reuptake and slowed cardiomyocyte relaxation were observed in adult cardiomyocytes with RAR α deletion, in consistent with these observations, downregulated expression of SERCA2a and decreased phosphorylation of PLB were demonstrated in RAR α KO mouse hearts or cardiomyocytes with RAR α deletion, which were rescued by overexpression of RAR α . These data suggest that decreased SR Ca²⁺ uptake activity due to

inhibited SERCA2a function is one of the main mechanisms in RAR α deletion-induced impairment of cardiomyocyte relaxation and diastolic dysfunction. RAR α deletion inhibited the phosphorylation of PLB, without affecting the total expression level of PLB, which resulted in increased PLB/SERCA2a ratio, leading to inhibition of the enzymatic activity of SERCA2a and impaired Ca²⁺ uptake. We observed that RAR α deletion-mediated inhibition of the phosphorylation of PLB was associated with decreased phosphorylation of CaMKII δ and Akt, and that activation of CaMKII or Akt abolished the inhibitory effect of RAR α deletion on PLB phosphorylation at Thr17. Though we did not determine the activation of PKA, RAR α deletion-induced decrease in phosphorylation of PLB at Ser16 was rescued by PKA activator. Furthermore, overexpression of RAR α prevented RAR α deletion-induced inhibition of the phosphorylation of CaMKII δ , Akt and PLB. These results suggest that RAR α signaling has an important role in regulation of PKA, CaMKII or Akt activity, which contribute to RAR α deletion-induced inhibition of phosphorylation of PLB and inactivation of SERCA2a. However, the mechanism of RAR α signaling in regulation of the activation of PKA, CaMKII or Akt in cardiomyocytes remains unclear.

Interestingly, we observed that the total expression level of CaMKII δ was significantly decreased following RAR α deletion, though the phosphorylation of CaMKII δ was relatively increased when compared to total CaMKII δ , the overall phosphorylation of CaMKII δ was reduced due to the decreased total protein level. These data suggest that decreased expression of CaMKII δ may have an important role in RAR α deletion-induced diastolic dysfunction, likely through the following mechanisms: (1) reducing the phosphorylation of PLB and inhibition of SERCA2a-mediated SR Ca²⁺ uptake, as we showed that increase in activation of CaMKII δ restored the decreased PLB phosphorylation level in response to RAR α deletion; (2) inhibiting the phosphorylation of titin, which is associated with the increased LV stiffness. Though we did not study the effect of RAR α deletion on titin protein, previous studies have shown that inhibition of CaMKII δ leads to deterioration in diastolic function through regulation of titin phosphorylation [58–60]. Most of studies have suggested that CaMKII-inhibition may be a therapeutic intervention for chronic overload-induced HF [61, 62]. However, our observation suggests that inhibition of CaMKII δ may be associated with the development of diastolic dysfunction. More studies are necessitated to clarify the role of RAR α in regulation of CaMKII δ and the association with which may provide a novel signaling mechanism for understanding how impaired RAR α signaling contributes to diastolic dysfunction and HF.

Oxidative stress plays an important pathogenic role in experimental and human heart failure. Increased ROS in the failing myocardium are mainly due to impaired antioxidant capacity, such as reduced activity of SOD and catalase, or stimulation of enzymatic sources, in which nonphagocytic NAD(P)H oxidases (NOX) are major enzymes responsible for production of O₂⁻. NOX2 and NOX4 are the predominant isoforms expressed in cardiomyocytes [63]. Studies have shown that NOX2 activation contributes to cardiomyocyte hypertrophy, fibrosis and heart failure through promoting oxidative stress and activation of MAP kinase pathway [64]. Evidence for a role of NOX4 in cardiac remodeling is contradictory, with considerable debate on whether NOX4 is protective or deleterious during cardiac response to injury [65, 66]. RAR α deletion-induced diastolic dysfunction is associated with significantly increased oxidative stress. Given the decreased SOD1 and SOD2 levels and increased expression of

NOX2 and NOX4, the increased production of ROS in cardiomyocytes with RAR α deletion is due to both impaired antioxidant ability to quench excess ROS, and NOX2/NOX4-mediated intracellular including mitochondria overproduction of ROS. Overexpression of RAR α in cardiomyocytes inhibited RAR α -deletion-induced increase in ROS generation, through inhibiting the expression of NOX2 and NOX4 and upregulating SOD1 and SOD2 levels, suggesting that impairment of RAR α signaling significantly contributes to the increased oxidative stress in myocardium. Redox-mediated activation of the MAP kinase pathways, mitochondrial death pathway and impaired SR calcium handling have been implicated in heart failure [67]. Oxidative stress may contribute to diastolic dysfunction by modification of RyRs, resulting in diastolic SR Ca²⁺ leaks and relaxation stiffness of cardiomyocytes [68]. The oxidation of CaMKII in response to ROS regulates relaxation through SERCA2a and activates the cell death pathway in cardiomyocytes [69, 70]. Redox-mediated SERCA2a sulfonation, on the cysteine residue, contributes to the impaired cardiomyocyte relaxation [71]. ROS-mediated inhibition of PKA activity may also have an important role in calcium mishandling [72]. RAR α deletion-induced impairment of Ca²⁺ uptake, decreased expression/activation of SERCA2a and the phosphorylation of PLB, CaMKII δ and Akt were rescued by anti-oxidant treatment or inhibition of NOX activation, suggesting that RAR α deletion-induced oxidative stress have a major role in calcium mishandling, through regulation of the activation of PKA, CaMKII δ or Akt, directly or indirectly, leading to dephosphorylation of PLB and inactivation of SERCA2a, which ultimately leads to impaired cardiomyocyte relaxation and diastolic dysfunction.

Systemic and myocardial (especially coronary microvascular endothelial) inflammation has been demonstrated to be an important pathophysiological mechanism for diastolic dysfunction in diastolic HF patients [73, 74]. Myocardial inflammation promotes oxidative stress in coronary microvascular endothelial cells, which limits NO bioavailability for adjacent cardiomyocytes. Impaired NO bioavailability suppresses cGMP-PKG-mediated signaling, which augments cardiomyocyte stiffness through hypophosphorylation of titin, resulting in diastolic dysfunction [75]. We observed increased oxidative stress in hearts of RAR α KO mice, and that RAR α deletion further promoted ROS generation in diabetic myocardium in STZ mice, which is associated with early development of diastolic dysfunction. We have previously reported that activation of RAR/RXR signaling inhibits metabolic stress-induced inflammatory responses and oxidative stress, through regulation of NF- κ B signaling [16, 17], suggesting that RAR/RXR-mediated inhibitory effect on myocardial inflammation and oxidative stress is involved in regulation of diastolic function. Though we did not directly identify the inflammatory responses following RAR α deletion in the present study, significantly increased ROS generation in RAR α KO or diabetic RAR α KO mice indirectly suggest the possible involvement of myocardial inflammation in the development of diastolic dysfunction. Further studies are necessary to understand the role of oxidative stress in regulation of NO/PKG signaling and titin expression/phosphorylation, and the association with RAR α deletion-induced diastolic dysfunction.

In conclusion, we have shown that myocardium specific deletion of RAR α in adult mouse results in diastolic dysfunction with preserved LVEF, and that downregulation of cardiac RAR α has a critical role in the development of diastolic dysfunction, in response to aging and metabolic stress. RAR α deletion-induced oxidative stress contribute significantly to

decreased expression/activation of SERCA2a and Ca²⁺ mishandling, which is directly associated with the impaired LV relaxation and diastolic dysfunction. Our findings highlight a novel mechanism that links nuclear RAR/RXR signaling to diastolic dysfunction, this will provide the impetus for generating effective therapeutic approaches to target RAR α -mediated signaling for the prevention and treatment of HF patients.

Supplementary Material

Refer to Web version on PubMed Central for supplementary material.

Acknowledgments

This material is the result of work supported with resources and the use of facilities at the Central Texas Veterans Health Care System, Temple, Texas.

Sources of Funding: This work was supported, in part, by a grant from the NIH (1R01 HL091902).

References

1. Steinberg BA, Zhao X, Heidenreich PA, Peterson ED, Bhatt DL, Cannon CP, et al. Trends in patients hospitalized with heart failure and preserved left ventricular ejection fraction: prevalence, therapies, and outcomes. *Circulation*. 2012; 126:65–75. [PubMed: 22615345]
2. Owan TE, Hodge DO, Herges RM, Jacobsen SJ, Roger VL, Redfield MM. Trends in prevalence and outcome of heart failure with preserved ejection fraction. *N Engl J Med*. 2006; 355:251–9. [PubMed: 16855265]
3. Boyer JK, Thanigaraj S, Schechtman KB, Perez JE. Prevalence of ventricular diastolic dysfunction in asymptomatic, normotensive patients with diabetes mellitus. *Am J Cardiol*. 2004; 93:870–5. [PubMed: 15050491]
4. Munzel T, Gori T, Keaney JF Jr, Maack C, Daiber A. Pathophysiological role of oxidative stress in systolic and diastolic heart failure and its therapeutic implications. *European heart journal*. 2015; 36:2555–64. [PubMed: 26142467]
5. Tsutsui H, Kinugawa S, Matsushima S. Oxidative stress and heart failure. *Am J Physiol Heart Circ Physiol*. 2011; 301:H2181–90. [PubMed: 21949114]
6. Ide T, Tsutsui H, Kinugawa S, Suematsu N, Hayashidani S, Ichikawa K, et al. Direct evidence for increased hydroxyl radicals originating from superoxide in the failing myocardium. *Circ Res*. 2000; 86:152–7. [PubMed: 10666410]
7. Myung SK, Ju W, Cho B, Oh SW, Park SM, Koo BK, et al. Efficacy of vitamin and antioxidant supplements in prevention of cardiovascular disease: systematic review and meta-analysis of randomised controlled trials. *BMJ*. 2013; 346:f10. [PubMed: 23335472]
8. Chambon P. A decade of molecular biology of retinoic acid receptors. *Faseb J*. 1996; 10:940–54. [PubMed: 8801176]
9. Guleria RS, Choudhary R, Tanaka T, Baker KM, Pan J. Retinoic acid receptor-mediated signaling protects cardiomyocytes from hyperglycemia induced apoptosis: role of the renin-angiotensin system. *J Cell Physiol*. 2011; 226:1292–307. [PubMed: 20945395]
10. Palm-Leis A, Singh US, Herbelin BS, Olsovsky GD, Baker KM, Pan J. Mitogen-activated protein kinases and mitogen-activated protein kinase phosphatases mediate the inhibitory effects of all-trans retinoic acid on the hypertrophic growth of cardiomyocytes. *J Biol Chem*. 2004; 279:54905–17. [PubMed: 15494319]
11. Zhou MD, Sucov HM, Evans RM, Chien KR. Retinoid-dependent pathways suppress myocardial cell hypertrophy. *Proc Natl Acad Sci U S A*. 1995; 92:7391–5. [PubMed: 7638203]
12. Wu J, Garami M, Cheng T, Gardner DG. 1,25(OH)₂ vitamin D₃ and retinoic acid antagonize endothelin-stimulated hypertrophy of neonatal rat cardiac myocytes. *J Clin Invest*. 1996; 97:1577–88. [PubMed: 8601621]

13. Wang HJ, Zhu YC, Yao T. Effects of all-trans retinoic acid on angiotensin II-induced myocyte hypertrophy. *J Appl Physiol.* 2002; 92:2162–8. [PubMed: 11960970]
14. Choudhary R, Baker KM, Pan J. All-trans retinoic acid prevents angiotensin II- and mechanical stretch-induced reactive oxygen species generation and cardiomyocyte apoptosis. *J Cell Physiol.* 2008; 215:172–81. [PubMed: 17941088]
15. Choudhary R, Palm-Leis A, Scott RC 3rd, Guleria RS, Rachut E, Baker KM, et al. All-trans retinoic acid prevents development of cardiac remodeling in aortic banded rats by inhibiting the renin-angiotensin system. *Am J Physiol Heart Circ Physiol.* 2008; 294:H633–44. [PubMed: 18156191]
16. Nizamutdinova IT, Guleria RS, Singh AB, Kendall JA Jr, Baker KM, Pan J. Retinoic acid protects cardiomyocytes from high glucose-induced apoptosis via inhibition of sustained activation of NF- κ B signaling. *J Cell Physiol.* 2013; 228:380–92. [PubMed: 22718360]
17. Guleria RS, Singh AB, Nizamutdinova IT, Souslova T, Mohammad AA, Kendall JA Jr, et al. Activation of retinoid receptor-mediated signaling ameliorates diabetes-induced cardiac dysfunction in Zucker diabetic rats. *J Mol Cell Cardiol.* 2013; 57C:106–18.
18. Thomas CM, Yong QC, Seqqat R, Chandel N, Feldman DL, Baker KM, et al. Direct renin inhibition prevents cardiac dysfunction in a diabetic mouse model: comparison with an angiotensin receptor antagonist and angiotensin-converting enzyme inhibitor. *Clin Sci (Lond).* 2013; 124:529–41. [PubMed: 23116220]
19. Rosas PC, Liu Y, Abdalla MI, Thomas CM, Kidwell DT, Dusio GF, et al. Phosphorylation of cardiac Myosin-binding protein-C is a critical mediator of diastolic function. *Circ Heart Fail.* 2015; 8:582–94. [PubMed: 25740839]
20. Sreejit P, Kumar S, Verma RS. An improved protocol for primary culture of cardiomyocyte from neonatal mice. *In Vitro Cell Dev Biol Anim.* 2008; 44:45–50. [PubMed: 18297366]
21. O'Connell TD, Rodrigo MC, Simpson PC. Isolation and culture of adult mouse cardiac myocytes. *Methods in molecular biology.* 2007; 357:271–96. [PubMed: 17172694]
22. Bers DM. Calcium fluxes involved in control of cardiac myocyte contraction. *Circ Res.* 2000; 87:275–81. [PubMed: 10948060]
23. Stammers AN, Susser SE, Hamm NC, Hlynsky MW, Kimber DE, Kehler DS, et al. The regulation of sarco(endo)plasmic reticulum calcium-ATPases (SERCA). *Can J Physiol Pharmacol.* 2015; 93:843–54. [PubMed: 25730320]
24. Haghighi K, Bidwell P, Kranias EG. Phospholamban interactome in cardiac contractility and survival: A new vision of an old friend. *J Mol Cell Cardiol.* 2014; 77:160–7. [PubMed: 25451386]
25. Catalucci D, Latronico MV, Ceci M, Rusconi F, Young HS, Gallo P, et al. Akt increases sarcoplasmic reticulum Ca²⁺ cycling by direct phosphorylation of phospholamban at Thr17. *J Biol Chem.* 2009; 284:28180–7. [PubMed: 19696029]
26. Simmerman HK, Collins JH, Theibert JL, Wegener AD, Jones LR. Sequence analysis of phospholamban. Identification of phosphorylation sites and two major structural domains. *J Biol Chem.* 1986; 261:13333–41. [PubMed: 3759968]
27. Tada M, Toyofuku T. Molecular regulation of phospholamban function and expression. *Trends in cardiovascular medicine.* 1998; 8:330–40. [PubMed: 14987547]
28. Wittmann T, Lohse MJ, Schmitt JP. Phospholamban pentamers attenuate PKA-dependent phosphorylation of monomers. *J Mol Cell Cardiol.* 2015; 80:90–7. [PubMed: 25562800]
29. Akin BL, Hurley TD, Chen Z, Jones LR. The structural basis for phospholamban inhibition of the calcium pump in sarcoplasmic reticulum. *J Biol Chem.* 2013; 288:30181–91. [PubMed: 23996003]
30. Toyoshima C, Asahi M, Sugita Y, Khanna R, Tsuda T, MacLennan DH. Modeling of the inhibitory interaction of phospholamban with the Ca²⁺ ATPase. *Proc Natl Acad Sci U S A.* 2003; 100:467–72. [PubMed: 12525698]
31. Kastner P, Grondona JM, Mark M, Gansmuller A, LeMeur M, Decimo D, et al. Genetic analysis of RXR alpha developmental function: convergence of RXR and RAR signaling pathways in heart and eye morphogenesis. *Cell.* 1994; 78:987–1003. [PubMed: 7923367]
32. Gruber PJ, Kubalak SW, Pexieder T, Sucov HM, Evans RM, Chien KR. RXR alpha deficiency confers genetic susceptibility for aortic sac, conotruncal, atrioventricular cushion, and ventricular muscle defects in mice. *J Clin Invest.* 1996; 98:1332–43. [PubMed: 8823298]

33. Lee RY, Luo J, Evans RM, Giguere V, Sucof HM. Compartment-selective sensitivity of cardiovascular morphogenesis to combinations of retinoic acid receptor gene mutations. *Circ Res.* 1997; 80:757–64. [PubMed: 9168777]
34. Leid M, Kastner P, Chambon P. Multiplicity generates diversity in the retinoic acid signalling pathways. *Trends Biochem Sci.* 1992; 17:427–33. [PubMed: 1333659]
35. Singh AB, Guleria RS, Nizamutdinova IT, Baker KM, Pan J. High Glucose-induced repression of RAR/RXR in cardiomyocytes is mediated through oxidative stress/JNK signaling. *J Cell Physiol.* 2012; 227:2632–44. [PubMed: 21882190]
36. Kraigher-Krainer E, Shah AM, Gupta DK, Santos A, Claggett B, Pieske B, et al. Impaired systolic function by strain imaging in heart failure with preserved ejection fraction. *J Am Coll Cardiol.* 2014; 63:447–56. [PubMed: 24184245]
37. Phan TT, Abozguia K, Nallur Shivu G, Mahadevan G, Ahmed I, Williams L, et al. Heart failure with preserved ejection fraction is characterized by dynamic impairment of active relaxation and contraction of the left ventricle on exercise and associated with myocardial energy deficiency. *J Am Coll Cardiol.* 2009; 54:402–9. [PubMed: 19628114]
38. Kass DA, Bronzwaer JG, Paulus WJ. What mechanisms underlie diastolic dysfunction in heart failure? *Circ Res.* 2004; 94:1533–42. [PubMed: 15217918]
39. Zile MR, Gottdiener JS, Hetzel SJ, McMurray JJ, Komajda M, McKelvie R, et al. Prevalence and significance of alterations in cardiac structure and function in patients with heart failure and a preserved ejection fraction. *Circulation.* 2011; 124:2491–501. [PubMed: 22064591]
40. Borlaug BA, Lam CS, Roger VL, Rodeheffer RJ, Redfield MM. Contractility and ventricular systolic stiffening in hypertensive heart disease insights into the pathogenesis of heart failure with preserved ejection fraction. *J Am Coll Cardiol.* 2009; 54:410–8. [PubMed: 19628115]
41. Su MY, Lin LY, Tseng YH, Chang CC, Wu CK, Lin JL, et al. CMR-verified diffuse myocardial fibrosis is associated with diastolic dysfunction in HFpEF. *JACC Cardiovasc Imaging.* 2014; 7:991–7. [PubMed: 25240451]
42. Kasner M, Westermann D, Lopez B, Gaub R, Escher F, Kuhl U, et al. Diastolic tissue Doppler indexes correlate with the degree of collagen expression and cross-linking in heart failure and normal ejection fraction. *J Am Coll Cardiol.* 2011; 57:977–85. [PubMed: 21329845]
43. Previs MJ, Beck Previs S, Gulick J, Robbins J, Warshaw DM. Molecular mechanics of cardiac myosin-binding protein C in native thick filaments. *Science.* 2012; 337:1215–8. [PubMed: 22923435]
44. Nagueh SF, Bachinski LL, Meyer D, Hill R, Zoghbi WA, Tam JW, et al. Tissue Doppler imaging consistently detects myocardial abnormalities in patients with hypertrophic cardiomyopathy and provides a novel means for an early diagnosis before and independently of hypertrophy. *Circulation.* 2001; 104:128–30. [PubMed: 11447072]
45. Poutanen T, Tikanoja T, Jaaskelainen P, Jokinen E, Silvast A, Laakso M, et al. Diastolic dysfunction without left ventricular hypertrophy is an early finding in children with hypertrophic cardiomyopathy-causing mutations in the beta-myosin heavy chain, alpha-tropomyosin, and myosin-binding protein C genes. *Am Heart J.* 2006; 151:725 e1–e9. [PubMed: 16504640]
46. Harris SP, Bartley CR, Hacker TA, McDonald KS, Douglas PS, Greaser ML, et al. Hypertrophic cardiomyopathy in cardiac myosin binding protein-C knockout mice. *Circ Res.* 2002; 90:594–601. [PubMed: 11909824]
47. Chen PP, Patel JR, Powers PA, Fitzsimons DP, Moss RL. Dissociation of structural and functional phenotypes in cardiac myosin-binding protein C conditional knockout mice. *Circulation.* 2012; 126:1194–205. [PubMed: 22829020]
48. Fraysse B, Weinberger F, Bardswell SC, Cuello F, Vignier N, Geertz B, et al. Increased myofilament Ca²⁺ sensitivity and diastolic dysfunction as early consequences of Mybpc3 mutation in heterozygous knock-in mice. *J Mol Cell Cardiol.* 2012; 52:1299–307. [PubMed: 22465693]
49. Wilder T, Ryba DM, Wieczorek DF, Wolska BM, Solaro RJ. N-acetylcysteine reverses diastolic dysfunction and hypertrophy in familial hypertrophic cardiomyopathy. *Am J Physiol Heart Circ Physiol.* 2015; 309:H1720–30. [PubMed: 26432840]

50. Figueiredo-Freitas C, Dulce RA, Foster MW, Liang J, Yamashita AM, Lima-Rosa FL, et al. S-Nitrosylation of Sarcomeric Proteins Depresses Myofilament Ca²⁺ Sensitivity in Intact Cardiomyocytes. *Antioxid Redox Signal*. 2015; 23:1017–34. [PubMed: 26421519]
51. Jia W, Shaffer JF, Harris SP, Leary JA. Identification of novel protein kinase A phosphorylation sites in the M-domain of human and murine cardiac myosin binding protein-C using mass spectrometry analysis. *J Proteome Res*. 2010; 9:1843–53. [PubMed: 20151718]
52. Sadayappan S, Gulick J, Osinska H, Barefield D, Cuello F, Avkiran M, et al. A critical function for Ser-282 in cardiac Myosin binding protein-C phosphorylation and cardiac function. *Circ Res*. 2011; 109:141–50. [PubMed: 21597010]
53. Schlender KK, Bean LJ. Phosphorylation of chicken cardiac C-protein by calcium/calmodulin-dependent protein kinase II. *J Biol Chem*. 1991; 266:2811–7. [PubMed: 1671569]
54. Tong CW, Stelzer JE, Greaser ML, Powers PA, Moss RL. Acceleration of crossbridge kinetics by protein kinase A phosphorylation of cardiac myosin binding protein C modulates cardiac function. *Circ Res*. 2008; 103:974–82. [PubMed: 18802026]
55. Schmidt U, Hajjar RJ, Helm PA, Kim CS, Doye AA, Gwathmey JK. Contribution of abnormal sarcoplasmic reticulum ATPase activity to systolic and diastolic dysfunction in human heart failure. *J Mol Cell Cardiol*. 1998; 30:1929–37. [PubMed: 9799647]
56. Kranias EG, Hajjar RJ. Modulation of cardiac contractility by the phospholamban/SERCA2a regulatome. *Circ Res*. 2012; 110:1646–60. [PubMed: 22679139]
57. Wold LE, Dutta K, Mason MM, Ren J, Cala SE, Schwanke ML, et al. Impaired SERCA function contributes to cardiomyocyte dysfunction in insulin resistant rats. *J Mol Cell Cardiol*. 2005; 39:297–307. [PubMed: 15878173]
58. Cheng J, Xu L, Lai D, Guilbert A, Lim HJ, Keskanokwong T, et al. CaMKII inhibition in heart failure, beneficial, harmful, or both. *Am J Physiol Heart Circ Physiol*. 2012; 302:H1454–65. [PubMed: 22287581]
59. Neef S, Sag CM, Daut M, Baumer H, Grefe C, El-Armouche A, et al. While systolic cardiomyocyte function is preserved, diastolic myocyte function and recovery from acidosis are impaired in CaMKII δ -KO mice. *J Mol Cell Cardiol*. 2013; 59:107–16. [PubMed: 23473775]
60. Hamdani N, Krysiak J, Kreuzer MM, Neef S, Dos Remedios CG, Maier LS, et al. Crucial role for Ca²⁺/calmodulin-dependent protein kinase-II in regulating diastolic stress of normal and failing hearts via titin phosphorylation. *Circ Res*. 2013; 112:664–74. [PubMed: 23283722]
61. Zhang T, Maier LS, Dalton ND, Miyamoto S, Ross J Jr, Bers DM, et al. The δ C isoform of CaMKII is activated in cardiac hypertrophy and induces dilated cardiomyopathy and heart failure. *Circ Res*. 2003; 92:912–9. [PubMed: 12676814]
62. Ling H, Zhang T, Pereira L, Means CK, Cheng H, Gu Y, et al. Requirement for Ca²⁺/calmodulin-dependent kinase II in the transition from pressure overload-induced cardiac hypertrophy to heart failure in mice. *J Clin Invest*. 2009; 119:1230–40. [PubMed: 19381018]
63. Zhang M, Perino A, Ghigo A, Hirsch E, Shah AM. NADPH oxidases in heart failure: poachers or gamekeepers? *Antioxid Redox Signal*. 2013; 18:1024–41. [PubMed: 22747566]
64. Parajuli N, Patel VB, Wang W, Basu R, Oudit GY. Loss of NOX2 (gp91phox) prevents oxidative stress and progression to advanced heart failure. *Clin Sci (Lond)*. 2014; 127:331–40. [PubMed: 24624929]
65. Zhao QD, Viswanadhapalli S, Williams P, Shi Q, Tan C, Yi X, et al. NADPH oxidase 4 induces cardiac fibrosis and hypertrophy through activating Akt/mTOR and NF κ B signaling pathways. *Circulation*. 2015; 131:643–55. [PubMed: 25589557]
66. Zhang M, Brewer AC, Schroder K, Santos CX, Grieve DJ, Wang M, et al. NADPH oxidase-4 mediates protection against chronic load-induced stress in mouse hearts by enhancing angiogenesis. *Proc Natl Acad Sci U S A*. 2010; 107:18121–6. [PubMed: 20921387]
67. Sorescu D, Griendling KK. Reactive oxygen species, mitochondria, and NAD(P)H oxidases in the development and progression of heart failure. *Congest Heart Fail*. 2002; 8:132–40. [PubMed: 12045381]
68. Terentyev D, Gyorke I, Belevych AE, Terentyeva R, Sridhar A, Nishijima Y, et al. Redox modification of ryanodine receptors contributes to sarcoplasmic reticulum Ca²⁺ leak in chronic heart failure. *Circ Res*. 2008; 103:1466–72. [PubMed: 19008475]

69. Erickson JR, Joiner ML, Guan X, Kutschke W, Yang J, Oddis CV, et al. A dynamic pathway for calcium-independent activation of CaMKII by methionine oxidation. *Cell*. 2008; 133:462–74. [PubMed: 18455987]
70. Palomeque J, Rueda OV, Sapia L, Valverde CA, Salas M, Petroff MV, et al. Angiotensin II-induced oxidative stress resets the Ca²⁺ dependence of Ca²⁺-calmodulin protein kinase II and promotes a death pathway conserved across different species. *Circ Res*. 2009; 105:1204–12. [PubMed: 19850941]
71. Qin F, Siwik DA, Lancel S, Zhang J, Kuster GM, Luptak I, et al. Hydrogen peroxide-mediated SERCA cysteine 674 oxidation contributes to impaired cardiac myocyte relaxation in senescent mouse heart. *Journal of the American Heart Association*. 2013; 2:e000184. [PubMed: 23963753]
72. Okatan EN, Tuncay E, Turan B. Cardioprotective effect of selenium via modulation of cardiac ryanodine receptor calcium release channels in diabetic rat cardiomyocytes through thioredoxin system. *J Nutr Biochem*. 2013; 24:2110–8. [PubMed: 24183307]
73. Paulus WJ, Tschope C. A novel paradigm for heart failure with preserved ejection fraction: comorbidities drive myocardial dysfunction and remodeling through coronary microvascular endothelial inflammation. *J Am Coll Cardiol*. 2013; 62:263–71. [PubMed: 23684677]
74. Franssen C, Chen S, Unger A, Korkmaz HI, De Keulenaer GW, Tschope C, et al. Myocardial Microvascular Inflammatory Endothelial Activation in Heart Failure With Preserved Ejection Fraction. *JACC Heart Fail*. 2016; 4:312–24. [PubMed: 26682792]
75. Kruger M, Kotter S, Grutzner A, Lang P, Andresen C, Redfield MM, et al. Protein kinase G modulates human myocardial passive stiffness by phosphorylation of the titin springs. *Circ Res*. 2009; 104:87–94. [PubMed: 19023132]

Highlight

- Cardiac specific gene deletion of RAR α induces diastolic dysfunction with preserved LVEF
- Loss of RAR α signaling promotes cardiac oxidative stress and calcium mishandling
- Oxidative stress plays a key role in SERCA2a inactivation and calcium mishandling in RAR α KO mice
- Cardiac expression of RAR α is downregulated in mice with metabolic stress or aging
- RAR α deletion accelerates metabolic stress-induced diastolic dysfunction

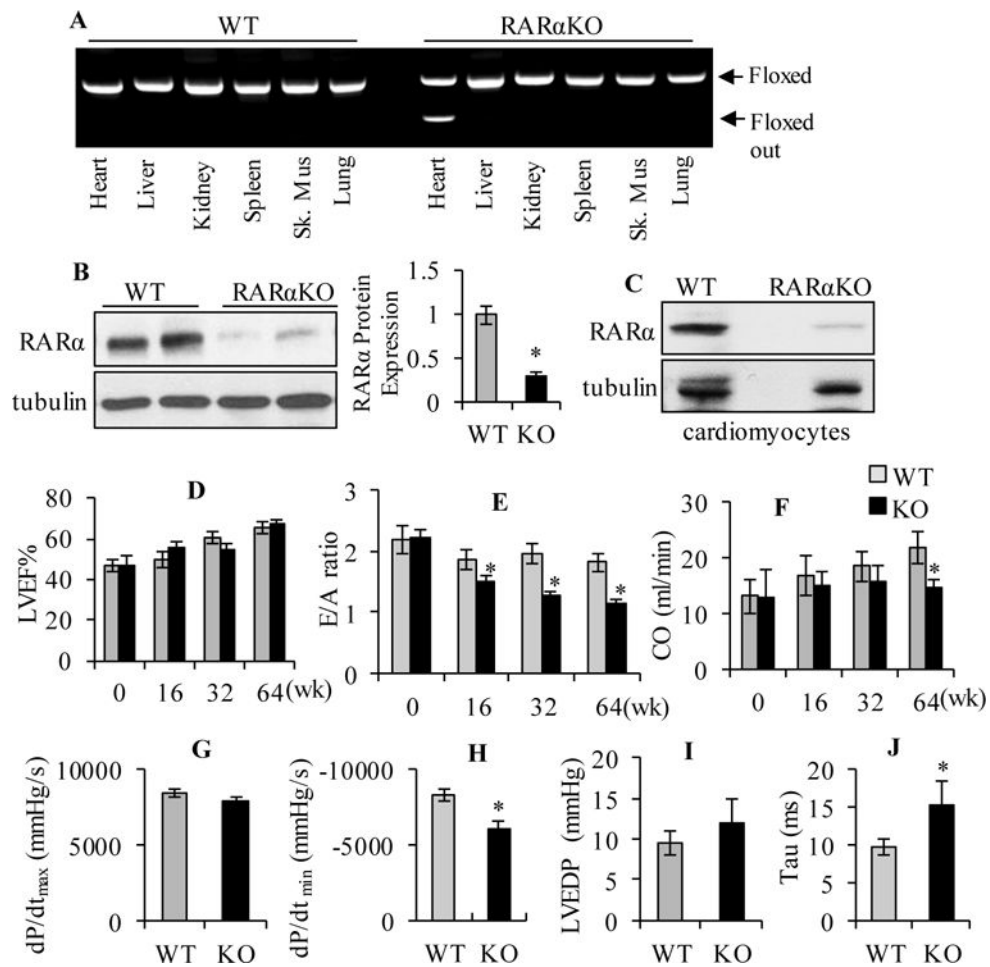


Fig. 1. Cardiac specific gene deletion of RAR α induces diastolic dysfunction
 (A) α -MHC-Cre-RAR $\alpha^{fl/fl}$ mice were treated with tamoxifen (0.5 mg/day) or vehicle for 4 days, at 6 wks of age, tissues were collected after 2 wks and PCR analysis of genomic DNA performed. Arrow indicates floxed and floxed out band. (B) Protein expression of RAR α in hearts of WT and RAR α KO mice, after 20 wks of gene deletion, was determined by Western blot and quantified by densitometry. * $p < 0.05$ vs WT. Equal loading was verified by α -tubulin expression. (C) Adult cardiomyocytes were isolated from WT and RAR α KO mice after 20 wks, protein expression of RAR α determined. (D–F) Echocardiography was performed at the times indicated, before (0) and after gene deletion. (D) LVEF%; (E) E/A ratio and (F) cardiac output (CO). * $p < 0.05$ vs age matched WT. (G–J) Cardiac catheterization was performed, dP/dt_{max} (G), dP/dt_{min} (H), LVEDP (I) and Tau (J) analyzed, in WT (n=10) and RAR α KO mice (n=9) at 20 wks. * $p < 0.05$ vs WT.

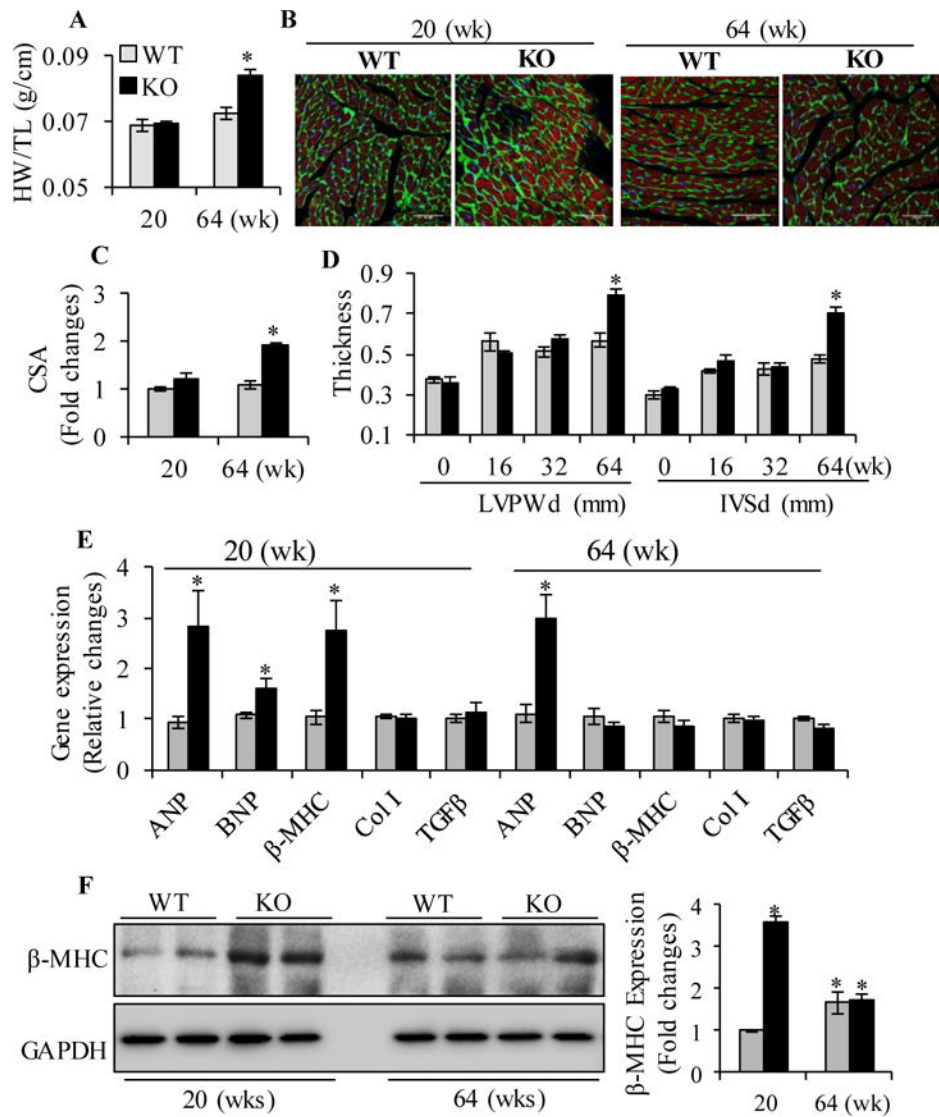


Fig. 2. Cardiac hypertrophic and fibrotic changes in *RARα*KO mice

(A) Heart weight/Tibia length (HW/TL) ratio. (B) Representative images of LV cardiomyocytes stained with wheat germ agglutinin (green), phalloidin (red) and DAPI (blue). Scale bars: 50 μ M. (C) Cardiomyocyte CSA was quantified from ~30 cardiomyocytes per section, 6 sections per group. * p <0.05 vs age matched WT. (D) Thickness of the end diastole LV posterior wall (LVPWd) and interventricular septum (IVSd) by echocardiography. * p <0.05 vs age matched WT. (E) Cardiac gene expression of ANP, BNP, β -MHC, Collagen type I (Col I) and TGF β in WT (n =10) and *RARα*KO mice (n =10). Data are mean value \pm SEM. * p <0.05 vs respective WT group. (F) Protein expression of β -MHC was determined in WT and *RARα*KO mice (n =6), at 20 and 64 wks, by Western blot and quantified by densitometry. Data are mean value \pm SEM. * p <0.05 vs WT at 20 wks.

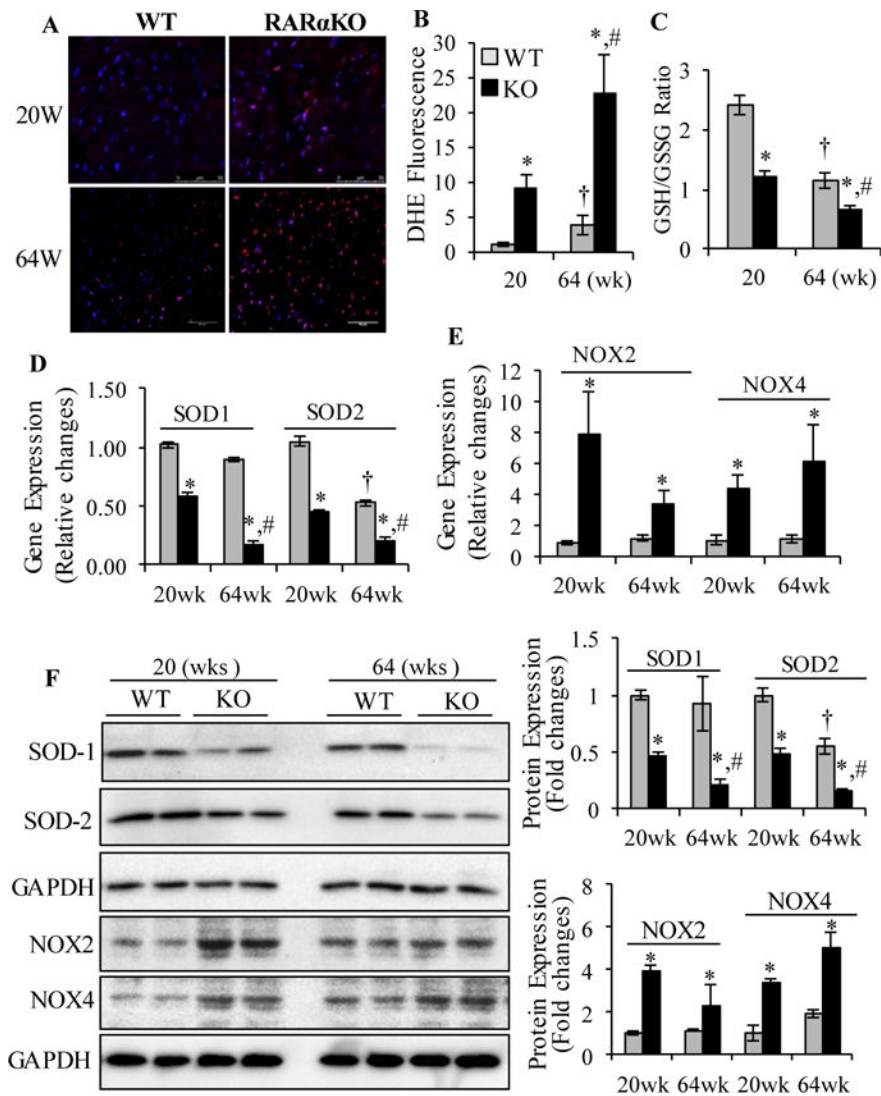


Fig. 3. Gene deletion of RAR α promotes cardiac oxidative stress

(A) Dihydroethidium (DHE) staining (red) of heart sections collected from WT and RAR α KO mice. Scale bars: 50 μ M. (B) DHE staining intensity was normalized to section area and plotted. (C) GSH/GSSG ratio. * p <0.05 vs age matched WT; † p <0.05 vs 20 wks WT; # p <0.05 vs 20 wks RAR α KO. Cardiac gene expression of SOD1, SOD2 (D) and NOX2 and NOX4 (E). Data are mean value \pm SEM (n =6). * p <0.05 vs age matched WT. † p <0.05 vs 20 wks WT; # p <0.05 vs 20 wks RAR α KO. (F) Protein expression of SOD1, SOD2, NOX2 and NOX4 was determined and quantified by densitometry. * p <0.05 vs age matched WT; † p <0.05 vs 20 wks WT; # p <0.05 vs 20 wks RAR α KO.

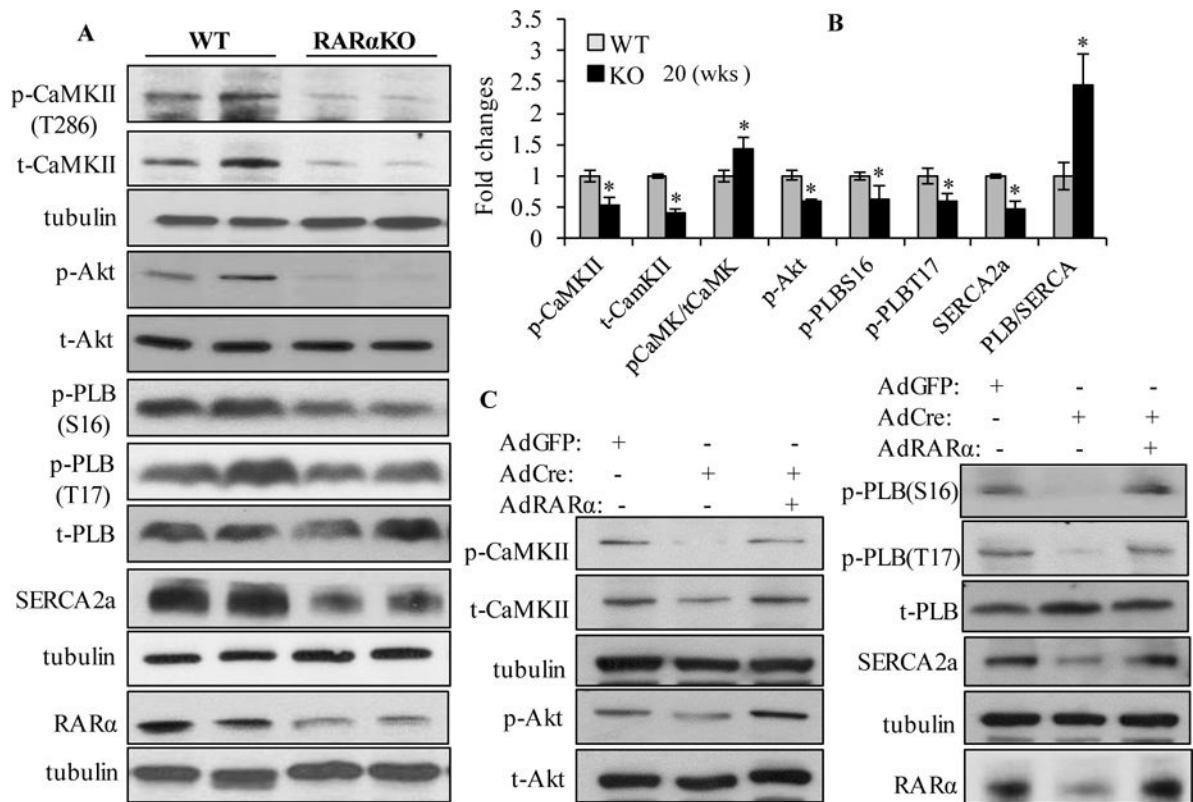


Fig. 4. Gene deletion of RAR α impairs calcium handling signaling

(A) Immunoblotting of total and/or phosphorylated CaMKII δ , Akt, PLB (~6 KD), SERCA2a and RAR α in the hearts of WT and RAR α KO mice, at 20 wks (n=6). Loading control was determined by α -tubulin expression. (B) Quantitative analysis of the data in (A).

*P<0.05 vs WT. (C) Neonatal cardiomyocytes isolated from RAR $\alpha^{fl/fl}$ mice were transfected with AdCre for 24 h, then transfected with or without AdRAR α . AdGFP transfected cells were used as control. Total and phosphorylated CaMKII δ , Akt, PLB, SERCA2a and RAR α were determined and quantified (Supplemental Fig. 7B).

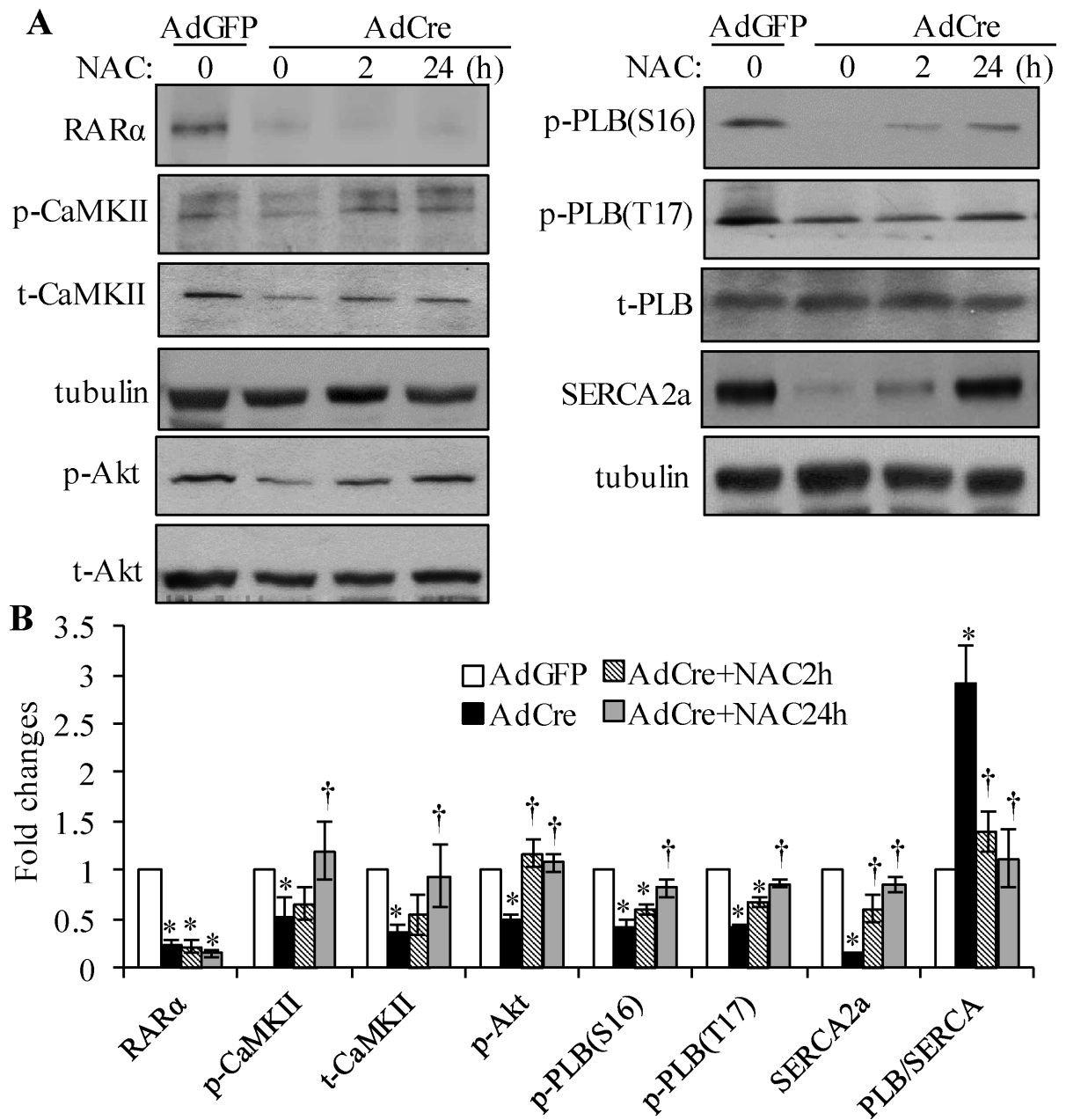


Fig. 5. Oxidative stress is involved in RAR α deletion-induced calcium mishandling

Neonatal mouse cardiomyocytes were transfected with AdGFP or AdCre, and then treated with or without N-acetyl-cysteine (NAC, 5 mmol/L) for 2 and 24 h, protein expression and phosphorylation of Akt, CaMKII δ , PLB, SERCA2a, RAR α and α -tubulin determined by Western blot (A) and quantified (B). * $p < 0.05$ vs AdGFP; † $p < 0.05$ vs AdCre.

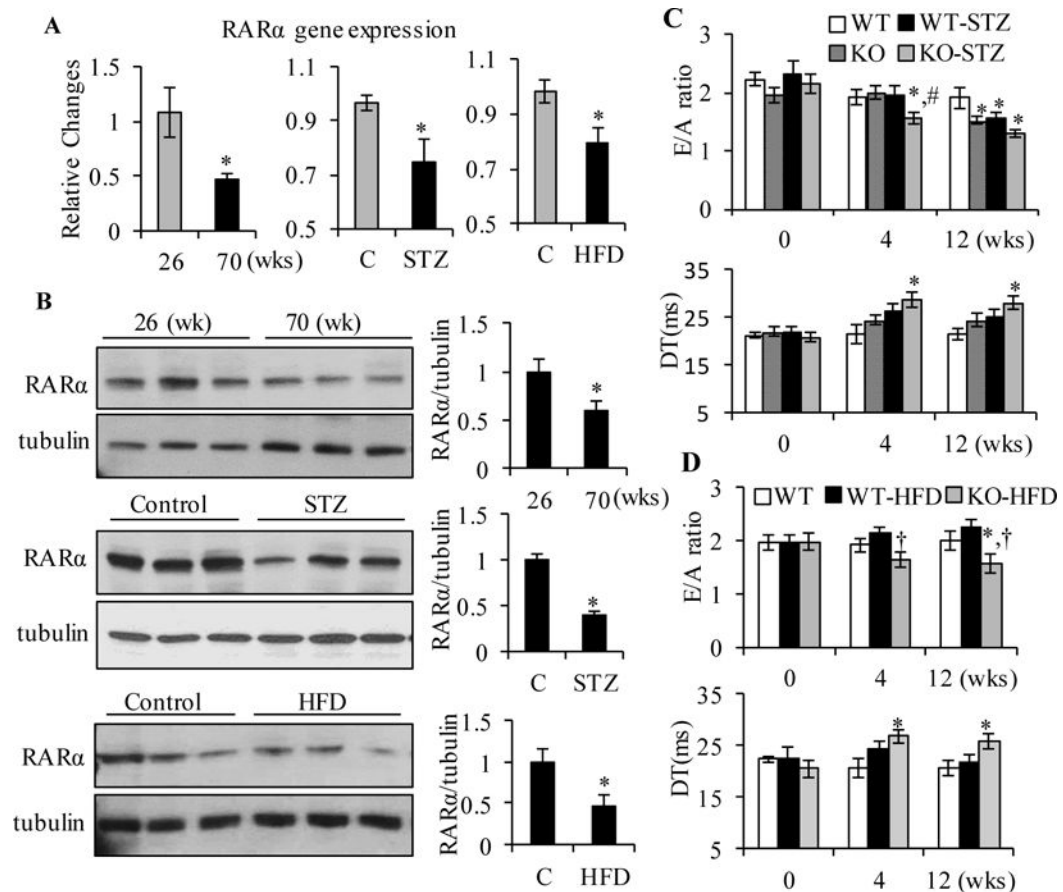


Fig. 6. Role of RAR α in regulation of metabolic stress-induced diastolic dysfunction
Gene (A) and protein (B) expression of RAR α was determined by real-time RT-PCR and Western blot, respectively, in hearts from young (26 wks old) and aged (70 wks old), control, STZ or HFD-fed mice (16 wks). * $p < 0.05$ vs young or control mice. E/A ratio and DT were analyzed by echocardiography in control, STZ-treated (C) or HFD-fed (D) WT and RAR α KO mice, at the times indicated. * $p < 0.05$ vs age matched WT, # $p < 0.05$ vs WT-STZ group; † $p < 0.05$ vs WT-HFD group.

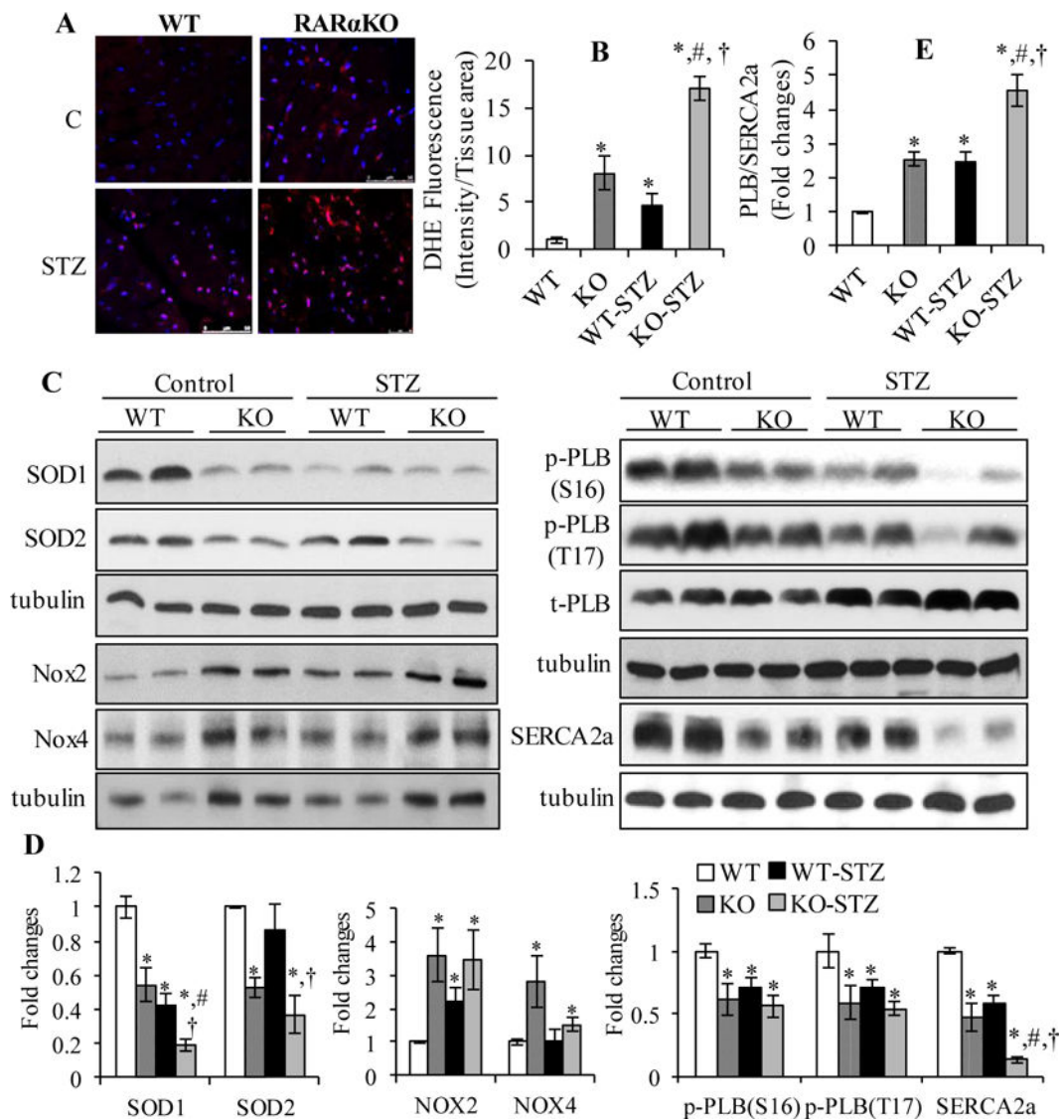


Fig. 7. Effect of RAR α deletion on cardiac oxidative stress and the expression of SERCA2a in STZ mice

(A) DHE staining (red) of heart sections in WT and RAR α KO mice, after 16 wks of STZ injection. Scale bar: 50 μ M. Staining intensity was normalized to section area and plotted (B). * p <0.05 vs WT; # p <0.05 vs RAR α KO; † p <0.05 vs WT-STZ group. (C) LV collected from control and STZ treated WT and RAR α KO mice, after 16 wks, protein expression of SOD1, SOD2, Nox2, Nox4, SERCA2a and phosphorylation of PLB was determined by Western blot and quantified by densitometry (D). (E) PLB/SERCA2a ratio. * p <0.05 vs WT; # p <0.05 vs RAR α KO; † p <0.05 vs WT-STZ.

Table 1Cell contractility and Ca²⁺ transients in cardiomyocytes from WT and RAR α .KO Mice

	WT (n=6)	RAR α .KO (n=7)	RAR α .KO+NAC (n=4)
Cell Contractility			
Peak shortening (%)	5.49±0.31	3.37±0.25*	3.81±0.16
+dL/dt (μm/s)	162.3±17.7	86.5±9.56*	134.8±10.6 [†]
-dL/dt (μm/s)	104.8±12.2	43.2±7.4*	89.3±13.1 [†]
TPS50% (s)	0.058±0.002	0.061±0.002	0.059±0.003
TPS90% (s)	0.096±0.006	0.106±0.006	0.098±0.006
TR50% (s)	0.236±0.016	0.293±0.018*	0.2446±0.026 [†]
TR90% (s)	0.411±0.028	0.669±0.052*	0.462±0.033 [†]
Tau (s)	0.135±0.009	0.196±0.013*	0.144±0.023 [†]
Ca²⁺ transients			
Baseline	1.121±0.019	1.145±0.012	1.148±0.017
dep v	2.354±0.174	2.422±0.142	2.387±0.502
dep v t	0.024±0.002	0.019±0.012	0.021±0.002
bl%peak h	6.538±0.445	6.569±0.477	6.333±1.095
T ₅₀ CI (s)	0.029±0.002	0.026±0.001	0.027±0.001
T ₉₀ CI (s)	0.052±0.002	0.048±0.001	0.049±0.001
SR load	0.502±0.041	0.449±0.036	0.476±0.042
ret v	0.658±0.060	0.397±0.017*	0.551±0.028 [†]
T50CR(s)	0.249±0.008	0.305±0.007*	0.274±0.007 [†]
T90CR (s)	0.546±0.034	0.805±0.052*	0.627±0.016 [†]
Tau (s)	0.242±0.009	0.358±0.014*	0.291±0.024 [†]

Adult cardiomyocytes isolated from WT and RAR α .KO mice after 20 wks of gene deletion, treated with or without NAC for 30 min. Cells were field stimulated, mechanical properties and intracellular Ca²⁺ transients were measured. NAC: N-acetyl-L-cysteine. For cell contractility: TPS50% and TPS90%: time to 50% and 90% of the peak shortening; TR50% and TR90%: time to 50% or 90% cell relengthening; Tau: the exponential decay time constant of the function. For Ca²⁺ transients: dep v: maximum velocities of Ca²⁺ transient ratio increase; T₅₀CI and T₉₀CI: time to 50% or 90% of Ca²⁺ transient ratio increase; ret v: maximum velocities of Ca²⁺ transient ratio recovery; T50CR and T90CR: time to 50% or 90% of Ca²⁺ transient ratio recovery; Tau: single exponential intracellular Ca²⁺ decay. Data are means ± SEM.

* P<0.05 vs WT;

[†] P<0.05 vs RAR α .KO.